Environmental Pollution 328 (2023) 121624

Contents lists available at ScienceDirect

Environmental Pollution

journal homepage: www.elsevier.com/locate/envpol

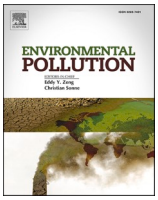

Bacterial benz(*a*)anthracene catabolic networks in contaminated soils and their modulation by other co-occurring HMW-PAHs☆

Sara N. Jiménez-Volkerink [a], Maria Jordán [a], David R. Singleton [b], Magdalena Grifoll [a,*], Joaquim Vila [a]

[a] Department of Genetics, Microbiology and Statistics, University of Barcelona, Av. Diagonal, 643, 08028, Barcelona, Spain
[b] Department of Civil and Environmental Engineering, Pratt School of Engineering, Duke University, Durham, NC, 27708-0287, USA

ARTICLE INFO

Keywords:
High molecular weight PAHs
Benz(*a*)anthracene
Biodegradation
DNA Stable Isotope Probing
Metagenomics
Microbial interactions

ABSTRACT

Polycyclic aromatic hydrocarbons (PAHs) are major environmental pollutants in a number of point source contaminated sites, where they are found embedded in complex mixtures containing different polyaromatic compounds. The application of bioremediation technologies is often constrained by unpredictable end-point concentrations enriched in recalcitrant high molecular weight (HMW)-PAHs. The aim of this study was to elucidate the microbial populations and potential interactions involved in the biodegradation of benz(*a*)anthracene (B*a*A) in PAH-contaminated soils. The combination of DNA stable isotope probing (DNA-SIP) and shotgun metagenomics of ^{13}C-labeled DNA identified a member of the recently described genus *Immundisolibacter* as the key B*a*A-degrading population. Analysis of the corresponding metagenome assembled genome (MAG) revealed a highly conserved and unique genetic organization in this genus, including novel aromatic ring-hydroxylating dioxygenases (RHD). The influence of other HMW-PAHs on B*a*A degradation was ascertained in soil microcosms spiked with B*a*A and fluoranthene (FT), pyrene (PY) or chrysene (CHY) in binary mixtures. The co-occurrence of PAHs resulted in a significant delay in the removal of PAHs that were more resistant to biodegradation, and this delay was associated with relevant microbial interactions. Members of *Immundisolibacter*, associated with the biodegradation of B*a*A and CHY, were outcompeted by *Sphingobium* and *Mycobacterium*, triggered by the presence of FT and PY, respectively. Our findings highlight that interacting microbial populations modulate the fate of PAHs during the biodegradation of contaminant mixtures in soils.

1. Introduction

Bioremediation is an accepted technology for the decontamination of soils impacted by polycyclic aromatic hydrocarbons (PAHs). However, its success is often constrained by end-point residues enriched in high molecular weight (HMW) PAHs exceeding regulatory limits. HMW PAHs, with 4 or more fused benzene rings, are of special concern due to their genotoxic and carcinogenic properties (Ghosal et al., 2016) and their potential bioaccumulation (van der Oost et al., 2003). Their low water solubility and high octanol/water partition coefficients limit their bioavailability, which, together with their chemical complexity and stability, hampers their microbial degradation in soils, providing them with long-term environmental persistence (Kanaly & Harayama, 2000). Although a number of soil bacterial strains have the capacity to mineralize HMW PAHs (Kanaly & Harayama, 2010), their biodegradation in polluted soils is assumed to be accomplished by the cooperation of different microbial populations undertaking interconnected metabolic pathways (Vila et al., 2015). Recent studies identifying previously unknown metabolites of HMW-PAHs in bioremediated soils highlight that the PAH biodegradation pathways inferred from the study of isolated strains may be only a part of the processes taking place (Tian et al., 2017, 2018). In soils, PAHs are embedded within complex mixtures (i.e., coal and crude oil derivatives) and interactions between the different components may be crucial in determining their individual fate, particularly that of HMW PAHs. Substrate interactions have been observed during the biodegradation of PAH mixtures by pure cultures and defined consortia (Mueller et al., 1989; Grifoll et al., 1995; Stringfellow & Aitken, 1995), revealing the relevance of cometabolic reactions as well as of competitive metabolism between PAHs (Bouchez et al., 1995). However, little is known about the potential interactions occurring during the

☆ This paper has been recommended for acceptance by Yucheng Feng.
* Corresponding author.
E-mail address: mgrifoll@ub.edu (M. Grifoll).

https://doi.org/10.1016/j.envpol.2023.121624
Received 22 December 2022; Received in revised form 4 April 2023; Accepted 9 April 2023
Available online 12 April 2023

biodegradation of PAH mixtures by complex soil microbial communities, where microbial synergism and/or competition may greatly influence the final composition of the HMW-PAH-enriched endpoint residue.

The bacterial biodegradation of benz(*a*)anthracene (B*a*A) has been addressed with pure cultures, especially with sphingomonads (Jerina et al., 1984; Sohn et al., 2004; Baboshin et al., 2008; Jouanneau et al., 2016) and mycobacteria (Kim et al., 2006). Most of these isolates could not grow on B*a*A as the sole carbon source, being only able to transform it as a result of the relaxed specificity of their aromatic ring-hydroxylating dioxygenases (RHD) and monooxygenases. This enzymatic promiscuity enables a single strain to attack B*a*A at multiple positions. For instance, the oxidation of B*a*A by *Sphingobium* sp. KK22 occurred via both the angular kata and linear kata ends of the molecule at the 1,2-, 3,4-, 8,9- and 10,11- positions (Kunihiro et al., 2013). *Mycobacterium vanbaalenii* PYR-1 preferentially hydroxylated B*a*A at the 10,11- positions but could also transform it at the 1,2- and 5,6- positions, giving the corresponding diols, and at the 7,12- positions, producing benz(*a*)anthracene-7,12-dione (Moody et al., 2005). However, information on the microbial populations and mechanisms that modulate the transformation and eventual mineralization of B*a*A in contaminated soils is still scarce.

In this study, we used B*a*A as a model HMW-PAH to understand the effect of substrate interactions during the degradation of this class of compounds in the complex soil matrix. First, we applied DNA-SIP using U^{13}C-benz(*a*)anthracene combined with shotgun metagenomic sequencing of ^{13}C-labeled DNA to identify the microbial populations and functions involved in B*a*A turnover in a PAH-contaminated soil. Second, we incubated soil microcosms spiked with B*a*A and three other HMW-PAHs (fluoranthene, pyrene and chrysene) individually or with B*a*A in binary mixtures with the others. By integrating biodegradation kinetics, metabolomic screens and 16S rRNA amplicon metagenomic sequencing data, we identified cosubstrate interferences that were associated with synergistic or antagonistic interactions within the soil microbiome.

2. Materials and methods

2.1. Chemicals

Benz(*a*)anthracene (B*a*A, 99%), fluoranthene (FT, >97%), pyrene (PY, 98%) and chrysene (CHY, 98%) were purchased from Sigma–Aldrich Chemie (Steinheim, Germany). Solvents (organic residue analysis grade) were obtained from J.T. Baker (Deventer, The Netherlands). Inorganic salts and other chemicals were acquired from Panreac Química S.A.U. (Barcelona, Spain) or Merck (Darmstad, Germany). Uniformly ^{13}C-labeled (U–^{13}C)-B*a*A was synthesized by methods described elsewhere (Zhang et al., 2011) and kindly provided by Z. Zhang and A. Gold.

2.2. Soil

The creosote-contaminated soil used in this study resulted from a previous lab-scale biostimulation treatment of heavily contaminated soil from a historical wood-treating facility in southern Spain. After 150 days of treatment with nutrients (urea and K_2HPO_4, C:N:P of 300:10:1) in aerobic conditions, the soil presented a Σ17 PAH content of 747 ± 95 mg/kg dry soil (Table S1). This treated soil was kept at 4 °C until use.

2.3. DNA-stable isotope probing (SIP) using U^{13}C-benz(a)anthracene

Incubations were conducted in 40-ml amber glass EPA vials with Teflon-lined stoppers containing 1 g of treated creosote-contaminated soil spiked with B*a*A (1 mg) supplied in acetone solution, as described by others (Jones et al., 2008). Two replicate vials were prepared for each incubation time point, and their whole content was used for residual B*a*A quantification. Two replicate flasks prepared in the same manner were acidified with phosphoric acid and used as killed controls to account for abiotic B*a*A losses at the end of the incubation. Soil moisture was adjusted to 40% WHC using sterile water supplemented with urea and K_2HPO_4 to meet a 300:10:1 C:N:P molar ratio relative to B*a*A carbon. Two additional sets of replicates were prepared in the same manner with unlabeled or [U–^{13}C]-benz(*a*)anthracene for SIP incubations that were incubated in parallel for the duration of the experiment. All vials were incubated statically at 25 °C in the dark. Further details on residual B*a*A quantification are provided in the Supplementary Material.

After significant B*a*A removal, soil from incubations in the presence of unlabeled or U^{13}C-labeled B*a*A was divided into portions containing approximately 250 mg (dry weight). Each 250-mg aliquot of soil was extracted using the DNeasy PowerSoil Kit (Qiagen, USA). DNA extracts from each 250-mg aliquot of a given replicate were combined and submitted to isopycnic ultracentrifugation on CsCl gradients. After centrifugation, 24 fractions of 250 μL each were collected from the bottom of each tube, and ^{13}C-enriched DNA was identified based on fraction density, DNA quantification and shifts in microbial communities based on DGGE analysis. DNA from ultracentrifuge fractions containing heavy DNA from a given replicate was pooled together to generate a 16S rRNA gene clone library for that replicate (for details, see Supplementary Material).

2.4. Shotgun metagenomic sequencing of ^{13}C-labeled DNA and analysis

Metagenome sequencing of ^{13}C-enriched DNA recovered from pooled fractions containing heavy DNA from one replicate SIP incubation was performed using an Illumina PE150 NovaSeq 6000 platform at Novogene Co. (Cambridge, UK). Adapter removal and quality filtering were performed on the received paired-end raw reads using Trimmomatic v.0.38 (Bolger et al., 2014) (ILLUMINACLIP:TrueSeq3-PE:2:30:10:8, LEADING:3 TRAILING:3, MINLEN:50, SLIDINGWINDOW:4:20, AVGQUAL:20). Raw read and trimmed read data quality was checked using FastQC (v0.11.8). Trimmed reads were assembled using metaSPAdes v3.9.0 (-meta option) (Nurk et al., 2017) and testing kmer sizes of 21, 33 and 55. Assembled scaffolds were clustered into bins with MaxBin2 v.2.2.7 (Wu et al., 2016) using trimmed reads for mapping and a minimum contig length of 1000 bp. The relative abundance of each bin was inferred by mapping reads to each bin with Bowtie2 v.2.4.2 (Langmead & Salzberg, 2012). Bin quality assessment was performed with CheckM v.1.0.18 (Parks et al., 2015) for contamination and completeness, and the bins were referred to as metagenome-assembled genomes (MAGs) when >90% completeness and <5% contamination. Taxonomic classification of the MAGs was performed using the Genome Taxonomy Database toolkit GTDB-Tk v.1.1.0 (Chaumeil et al., 2020). Functional annotation of the most abundant and complete MAGs was performed using Prokka v.1.14.6 (Seemann, 2014). The GhostKOALA annotation server was used to reconstruct metabolic pathways. The presence of genes related to PAH metabolism was assessed using Prokka, RAST and KEGG annotation and searches against the AromaDeg database (Duarte et al., 2014).

2.5. BaA biodegradation in soil microcosms in the presence of HMW-PAHs as cosubstrates

The treated creosote-polluted soil was used as inoculum (10% w/w) for soil microcosms containing sterile agricultural soil spiked with B*a*A, FT, PY or CHY individually or in binary mixtures of B*a*A with the other PAHs as cosubstrates (B*a*A + FT, B*a*A + PY or B*a*A + CHY). The final concentration of each of the spiked PAHs in the microcosms was 200 ppm. For each condition, triplicate microcosms were set up consisting of hermetic glass jars containing 70 g of soil with the water content adjusted to 40% of its WHC. Microcosms (27 in total) were incubated for 60 days at 25 °C in the dark. Before set-up, the agricultural soil was homogenized by sieving through a 2 mm mesh and mixing and was submitted to four cycles of autoclave sterilization (45 min, 121 °C)

separated by 24 h intervals. Effective soil sterilization was verified by negative results in MPN counts using R2 medium. After 0, 15, 30, 45 and 60 days, the content of each jar was homogenized, and samples were collected for chemical (5 g stored at −20 °C) and molecular analysis (1 g stored at −80 °C). Further details on chemical analysis (quantification of residual PAHs), DNA and RNA extraction, and cDNA synthesis are provided in the Supplementary Material.

2.6. 16S rRNA amplicon metagenomic sequencing

Triplicate DNA samples from microcosm incubations at selected data points (0, 15 and 30 days) were submitted to 16S rRNA amplicon sequencing. Paired-end reads (2 × 250 bp) of the V4 region of the 16S rRNA gene were obtained using primers 515F/806R (Caporaso et al., 2011) and Illumina NovaSeq equipment and reagents at Novogene Co. (Cambridge, UK). The received raw data were processed using mothur 1.45.3 following the MiSeq standard operating procedure (Kozich et al., 2013, last accessed June 2021). 16S rRNA gene libraries produced a total of 3,762,443 quality sequences with an average of 62,009 reads per sample. Sequences were aligned using SILVA v138 (Quast et al., 2013) reference files and clustered into operational taxonomic units (OTUs) using a 99% sequence identity cutoff. The OTU taxonomic affiliations were assigned to each representative sequence using the Ribosomal Database Project (RDP) database v9 (Cole et al., 2014). Rarefaction curves, library coverages and α-diversity indices (Simpson's inverse index) were estimated by normalizing the number of reads/sample to that of the least represented sample (52,825 reads). Representative sequences for each OTU were obtained using the get.oturep command in mothur (Schloss et al., 2009). Linear discriminant analysis effect size (LEfSe) was performed on the Galaxy server with default settings to determine the OTUs most likely to explain differences between incubation conditions (Segata et al., 2011).

2.7. Quantitative PCR (qPCR) amplification

The quantitative evolution of the bacterial community present in the microcosms was monitored by real-time PCR (qPCR). Total bacterial populations (DNA) and total active bacterial populations (cDNA) were quantified by amplification of the 16S rRNA gene using universal primers 341F and 534R (Muyzer et al., 1993). The most relevant bacterial populations identified during the metagenomic 16S rRNA amplicon sequencing analysis were monitored by qPCR using specific primers targeting their 16S rRNA gene sequence. The selected phylotypes were *Immundisolibacter*, *Pseudoxanthomonas*, *Mycobacterium* and *Sphingobium*. qPCR was conducted on an Applied Biosystems StepOne Real-Time PCR system (Applied Biosystems, USA) and further analyzed using StepOne Software v.2.3 (Applied Biosystems). Reactions with a total volume of 20 μL were prepared in 96-well plates containing PowerUp SYBR Green Master Mix (Applied Biosystems, CA, USA), 1 μL of template and 4 pmol of each primer. The primer pairs and conditions used for each determination are described in Table S2. Primer specificities were validated *in silico* by using NCBI Primer-BLAST and tested experimentally by PCR amplification on DNA and cDNA samples containing the target sequence. Quantification was achieved against a standard calibration curve of 8 points. Standards were obtained by cloning almost full-length 16S rRNA gene fragments using a pGEM-T Easy Vector System (Promega, Madison, USA). For total bacterial quantification, a fragment of the 16S rRNA gene of *E. coli* CECT 101 was used. For reactions targeting specific phylotypes, we used plasmids recovered from clone library analyses performed in previous experiments. All qPCRs had an efficiency ranging between 85% and 110% and a slope between −3.2 and −3.8. Primer specificity was also assessed by the observation of a single peak during melt curve analysis.

2.8. Statistical analysis

Data were subjected to analysis of variance (ANOVA) and Tukey's *post hoc* test for multiple comparisons in IBM SPSS Statistics v.23 software, with mean differences significant at $P < 0.05$.

2.9. Data availability

Shotgun metagenomics and 16S rRNA gene amplicon data from the SIP experiment and the soil microcosms can be found at NCBI under BioProject PRJNA894976. The Whole Genome Shotgun project has been deposited at DDBJ/ENA/GenBank under the accession JAPRBE000000000. The metagenome assembled genome (MAG) for *Immundisolibacter* sp. BA1 has been deposited under accession number JAQRGD000000000. The 16 S rRNA gene sequences from the clone library of the SIP experiment can be found in GenBank under accession numbers OP782700-OP782703.

3. Results and discussion

3.1. Identification of the BaA-degrading community by DNA-SIP combined with shotgun metagenomics

After effective B*a*A removal (35% of the initial concentration), fractions containing ^{13}C-enriched DNA were identified based on DNA quantification and shifts in bacterial community profiles by DGGE analysis. In U–^{13}C-B*a*A incubations, the DGGE patterns revealed a shift in four fractions (density ranging from 1.735 to 1.745 mg L^{-1}), showing a dramatic enrichment of one particular band (Fig. S1). In incubations with unlabeled B*a*A, DNA was not recovered from the corresponding fractions. Fractions corresponding to light DNA in incubations with U–^{13}C-B*a*A showed a similar microbial community composition to those with unlabeled substrate. Therefore, the four DNA fractions with greater density and clear community shifts were pooled together and considered ^{13}C-enriched DNA.

The vast majority of sequences (84%) in the 16S rRNA gene clone library obtained from heavy DNA were related to a member of *Immundisolibacter* (Table S3), thus identifying this phylotype (BA1) as a major player in the utilization of B*a*A in this soil. This gammaproteobacterial genus, described after the recent isolation of strain *Immundisolibacter cernigliae* TR3.2 (Corteselli et al., 2017), had previously been related to the degradation of anthracene, fluoranthene, pyrene and benz(*a*)anthracene using DNA-SIP on a manufactured gas plant soil from North Carolina (Jones et al., 2011). Other less abundant phylotypes detected in the heavy DNA clone libraries corresponded to members of *Sphingobium* (10%), *Olivibacter* (4%) and *Achromobacter* (2%). *Sphingobium* BA2 shared a high 16S rRNA gene sequence identity (>99%) with *Sphingobium* strains isolated from contaminated environments, for instance, the hexachlorocyclohexane-degrading *S. ummariense* RL-3 (Accession number: NR_044171; Singh & Lal, 2009), the bisphenol A-degrading *Sphingobium* sp. SO1a (AB453305; Matsumura et al., 2009), and *S. cloacae* LH227, able to grow on phenanthrene and biotransform other PAHs (AY151393; Bastiaens et al., 2000). The catabolic versatility of this genus and the fact that members of *Sphingobium* have shown the ability to transform B*a*A (Kunihiro et al., 2013) suggest that phylotype BA2 could also be involved in B*a*A utilization, but to a minor extent compared to *Immundisolibacter* BA1. For *Olivibacter* and *Achromobacter,* their low sequence abundance in the clone library and the 16S rRNA sequence similarity (>99%) to rhizospheric (NR_041503, KR055002) and plant endophytic (KF844050, KR055002) bacteria from pristine environments suggest that they could be growing on intermediate metabolites of B*a*A produced by primary degraders.

Shotgun metagenomic sequencing of ^{13}C-enriched DNA generated a total of 25.9 million quality-filtered paired-end reads that were assembled into 46,337 contigs (largest contig 102,172 bp, N50 1874 bp) and binned into 13 metagenomic bins (Table S4). Only bins with >90%

completeness and <5% contamination were considered metagenome-assembled genomes (MAGs). As expected, the most abundant MAG (72.7% relative abundance) corresponded to *Immundisolibacter*, most closely related to the type strain *Immundisolibacter cernigliae* (GCF_001697225.1, 94.34% ANI). Another less abundant MAG belonged to a member of *Pseudoxanthomonas* (bin 2, 4.8%). Although presenting a low-quality value, an almost complete genome corresponded to *Sphingobium* (bin 3, 3.3%). Along these, many other incomplete and low-quality bins were assembled (bins 4–10). No MAGs were related to either *Olivibacter* or *Achromobacter*, as would have been expected from the 16S rRNA clone library. Nevertheless, partial 16S rRNA sequences recovered from the shotgun metagenomic sequencing included members of *Immundisolibacter*, *Sphingobium* and *Olivibacter*, showing 100% identity to sequences retrieved from the clone library from the DNA-SIP incubations.

3.2. Functional analysis of *Immundisolibacter* sp. BA1 metagenome-assembled genome

Considering its key role in the biodegradation of B*a*A, a metagenomic functional gene analysis of the *Immundisolibacter* sp. BA1 MAG was conducted. The annotated *Immundisolibacter* sp. BA1 MAG presented 2613 CDSs, 48 tRNA genes and 4 rRNA genes, including a partial 16S rRNA gene sequence with 100% identity to the corresponding clone library sequence. Functional gene annotation revealed a large repertoire of dioxygenases and monooxygenases with potential activity on aromatic compounds (Table S5). Genes coding for aromatic ring-hydroxylating dioxygenases (RHD) were grouped according to Prokka annotation and phylogenetic analysis of the amino acid sequences (Fig. S2). The *Immundisolibacter* sp. BA1 MAG presented a vast number of aromatic RHD coding genes, including putative naphthalene/biphenyl/benzene dioxygenases, benzoate/p-cumate dioxygenases, salicylate hydroxylases/anthranilate/terephthalate dioxygenases and carbazole dioxygenases.

Further elucidation of the functional annotation of the *Immundisolibacter* sp. BA1 MAG revealed the presence of a catabolic gene cluster composed of genes coding for 7 different α-subunits of RHD, 5 RHD β-subunits, 2 aromatic ring-cleaving dioxygenases (one β-subunit of a protocatechuate dioxygenase (*LigB*) and one biphenyl-2,3-diol dioxygenase) and one hydrolase involved in aromatic metabolism (Fig. 1). The gene cluster also included a TetR/AcrR family transcriptional regulator, along with a couple of hypothetical proteins. Strikingly, a gene cluster with the exact same configuration was found to be enclosed in the genome of the HMW-PAH-degrading *Immundisolibacter cernigliae* TR3.2 (Singleton et al., 2016), both sharing a high nucleotide identity (78–98%). Furthermore, a functional metagenomic screening using fosmid libraries from a PAH-contaminated soil from the Czech Republic subjected to 12 years of *in situ* bioremediation (Duarte et al., 2017) also revealed the presence of resembling gene clusters. The detection of conserved genetic organizations encoding enzymes crucial for PAH biodegradation in members of *Immundisolibacter* untaps a common trait for the metabolism of PAHs within this scarcely characterized genus.

BLAST analysis of the amino acid sequences of the α-subunits of potential PAH-RHD from the *Immundisolibacter* sp. BA1 MAG revealed that they were closely related to RHDs found in hydrocarbon-contaminated sites from diverse geographic locations (Table S6). The widespread distribution of these RHDs suggests the crucial role of the genus *Immundisolibacter* in the biodegradation of polyaromatic hydrocarbons in soils. A phylogenetic analysis of the 6 amino acid sequences annotated as α-subunits of naphthalene/biphenyl/benzene dioxygenases (BAA_00138, BAA_00433, BAA_00933, BAA_02333, BAA_02435, BAA_02437) shows that most of these enzymes are distantly related to other well-known RHDs (Fig. 2). It is worth noting a separate branch in the phylogenetic tree, comprised of sequences for RHD mainly found in members of *Immundisolibacter*, including one of the RHD present in the aforementioned gene cluster (BAA_00433), suggesting the existence of a novel group of PAH-RHD distantly related to those present in other bacteria. Interestingly, neither of the RHDs from *Immundilsolibacter* sp. BA1 included in this branch (BAA_00138, BAA_00433) were detected by the Aromadeg database. These findings highlight the potential of functional screening of metagenomic data for the identification of novel aromatic-degradation genes, untapping uncharacterized features not previously reported from isolates or PCR-based screens.

Considering the number of RHD genes in the *Immundisolibacter* sp. BA1 MAG, it is difficult to predict which genes encode the enzymes catalyzing the biodegradation of B*a*A. In a previous study applying stable isotope-assisted metabolomics using ^{13}C-labeled B*a*A, the authors reconstructed the B*a*A biotransformation pathway in this soil (Tian et al., 2018). B*a*A biodegradation mainly followed the metabolic pathway previously described for *Sphingobium yanoikuyae* strains B8/83 and B1 (Jerina et al., 1984; Mahaffey et al., 1988), initiated by dioxygenation at positions 1 and 2, followed by *meta* cleavage leading to the formation of 1-hydroxy-2-anthracenoic acid, an intermediate also observed in *Sphingobium* sp. KK22 (Kunihiro et al., 2013). The route would continue with further oxidation to a dihydrodiol, followed by dehydrogenation and ring cleavage to produce two different isomers of dihydroxynaphthalene dicarboxylic acid. Although this pathway was proposed during an active bioremediation process of the creosote-contaminated soil, our results would link it to *Immundisolibacter* sp. BA1, identified as the primary B*a*A-degrading bacterium. Interestingly, the MAG possessed all of the genes necessary for downstream biotransformation of 1,2-dihydroxynaphthalene (*nahC*, *nahD* and *nahD*) and *cis*-2,3-dihydrobiphenyl-2,3-diol (*bphB*, *bphC* and *bphD*). The GhostKOALA annotation also showed that *Immundisolibacter* sp. holds the complete catechol *meta*-cleavage pathway (*xylEFGHIJ*), harboring 4 different genes coding for catechol 2,3-dioxygenases, suggesting that the B*a*A metabolic pathway might proceed via catechol. Moreover, the lack of genes encoding gentisate 1,2-dioxygenase supports the hypothesis that salicylate would be channeled via catechol, probably by the action of proteins annotated as anthranilate 1,2-dioxygenases (Jouanneau et al., 2007).

3.3. Influence of HMW-PAH cosubstrates on B*a*A biodegradation kinetics

At the end of the incubation, the soil microcosms spiked with single PAHs showed extensive degradation of B*a*A (95.3%), FT (96.5%), PY (96.2%) and CHY (72.8%). When coincubated, B*a*A showed a slightly lower degradation extent (92.1% with FT, 84.3% with PY and 91.8% with CHY), although the differences were not significant. For the PAHs supplied as cosubstrates, neither FT nor PY degradation seemed to be affected by the presence of B*a*A, showing degradation extents comparable to those observed in single-substrate incubations (96.1% and 97.3%, respectively). In the case of CHY, however, the presence of B*a*A seemed to stimulate its degradation, as the final concentration of CHY was significantly lower than that in single-substrate incubation (80.1%).

Conversely, the presence of cosubstrates had major effects on the degradation kinetics of certain PAHs (Fig. 3). When incubated alone, B*a*A showed typical “hockey stick” kinetics with maximum biodegradation rates during the first 30 days (22.1 ± 0.1 nmol kg^{-1}·day^{-1}). In the presence of FT or PY, B*a*A degradation was significantly delayed and started only after 15 days of incubation, when FT or PY had already been removed. Afterward, the B*a*A concentration was rapidly depleted between 15 and 30 days, showing significantly higher maximum rates compared to incubations with B*a*A alone (41.4 ± 0.9 nmol kg^{-1}·day^{-1} with FT and 37.3 ± 2.8 nmol kg^{-1}·day^{-1} with PY). The biodegradation kinetics of FT and PY remained identical with or without the presence of B*a*A, being almost completely removed during the first 15 days of incubation with rapid rates (51.3 ± 0.8 nmol kg^{-1}·day^{-1} FT[+B*a*A]; 53.8 ± 0.7 nmol kg^{-1}·day^{-1} FT; 46.3 ± 0.5 nmol kg^{-1}·day^{-1} PY[+B*a*A]; 48.3 ± 0.3 nmol kg^{-1}·day^{-1} PY). When B*a*A and CHY were coincubated, the rate of B*a*A did not suffer significant changes in comparison to the single-substrate incubation. In contrast, CHY utilization was delayed by

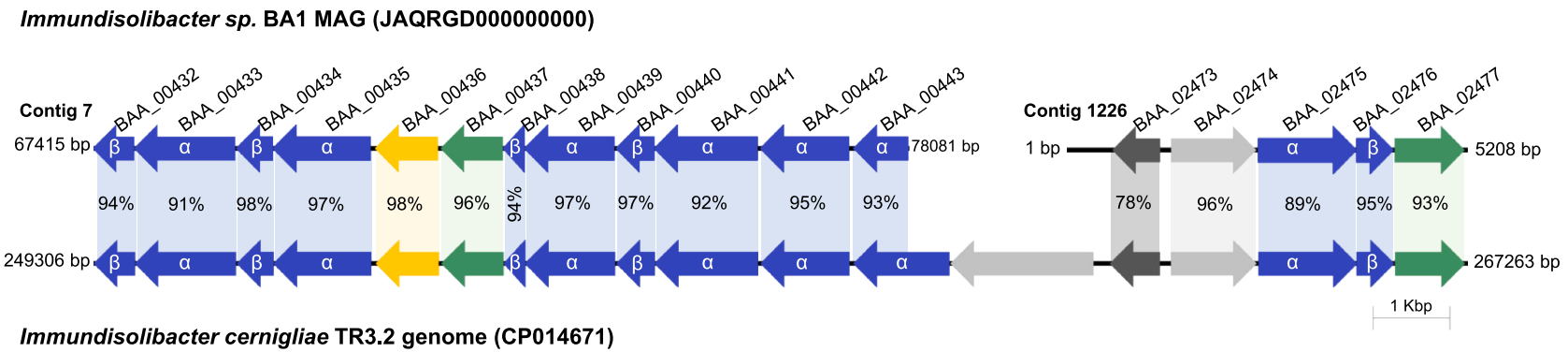

Locus tag	Contig	Start	End	Strand	Length (bp)	Annotation
BAA_00432	7	67415	67957	-	543	Biphenyl 2,3-dioxygenase subunit beta
BAA_00433	7	67954	69279	-	1326	Benzene 1,2-dioxygenase subunit alpha
BAA_00434	7	69291	69770	-	480	p-cumate 2,3-dioxygenase system, small oxygenase component
BAA_00435	7	69770	71047	-	1278	Anthranilate 1,2-dioxygenase large subunit
BAA_00436	7	71106	71930	-	825	2-hydroxy-6-oxo-6-(2'-aminophenyl)hexa-2,4-dienoic acid hydrolase
BAA_00437	7	71964	72779	-	816	Protocatechuate 4,5-dioxygenase beta chain
BAA_00438	7	72781	73062	-	282	Small subunit meta-cleavage dioxygense
BAA_00439	7	73059	74237	-	1179	Carbazole 1,9a-dioxygenase, terminal oxygenase component CarAa
BAA_00440	7	74256	74759	-	504	2-halobenzoate 1,2-dioxygenase small subunit
BAA_00441	7	74756	76111	-	1356	2-halobenzoate 1,2-dioxygenase large subunit
BAA_00442	7	76144	77307	-	1164	Carbazole 1,9a-dioxygenase, terminal oxygenase component CarAa
BAA_00443	7	77362	78081	-	720	Anthranilate 1,2-dioxygenase large subunit
BAA_02473	1226	595	1221	-	627	TetR/AcrR family transcriptional regulator
BAA_02474	1226	1366	2481	+	1116	hypothetical protein
BAA_02475	1226	2505	3794	+	1290	p-cumate 2,3-dioxygenase system, large oxygenase component
BAA_02476	1226	3791	4279	+	489	p-cumate 2,3-dioxygenase system, small oxygenase component
BAA_02477	1226	4291	5208	+	918	Biphenyl-2,3-diol 1,2-dioxygenase

Fig. 1. Genetic organization of the PAH-degrading gene cluster of *Immundisolibacter* sp. BA1 metagenome-assembled genome (MAG) compared to the corresponding gene cluster in the *Immundisolibacter cernigliae* TR3.2 genome. Percentages represent nucleotide sequence identity. In blue, aromatic ring-hydroxylating dioxygenases; in green, aromatic ring-cleavage dioxygenases; in yellow, enzymes of the lower aromatic pathway; in dark gray, transcriptional regulators; in light gray, hypothetical proteins. Annotation of the genes conforming the cluster are listed in the table (Prokka v.1.14.6). (For interpretation of the references to colour in this figure legend, the reader is referred to the Web version of this article.)

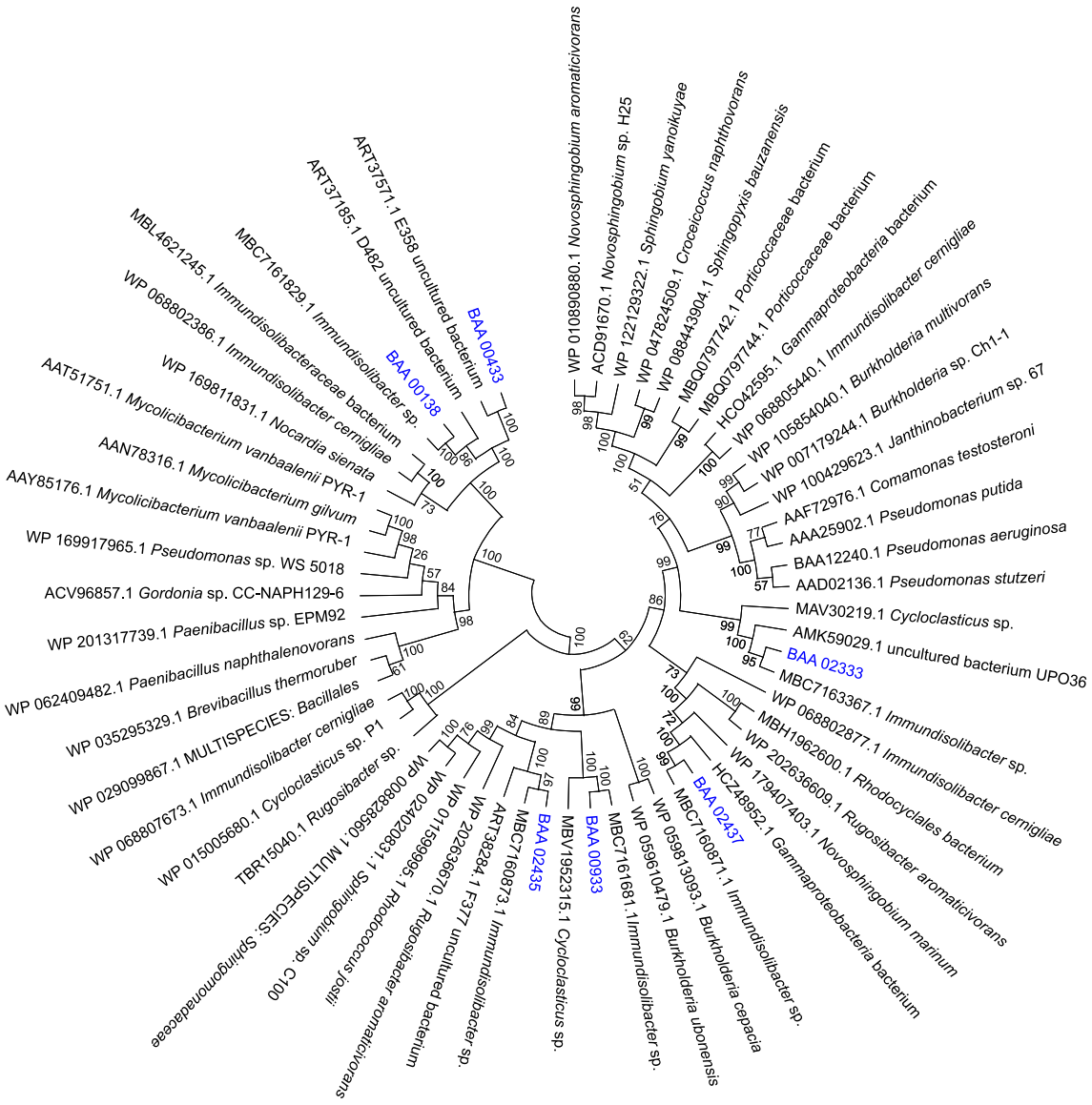

Fig. 2. Phylogenetic tree of the alpha subunits of aromatic ring-hydroxylating dioxygenases (RHD) using the maximum-likelihood method of amino acid sequences from the *Immundisolibacter* sp. BA1 metagenome assembled genome (MAG) (in blue). Reference sequences corresponding to the closest RHD protein sequences and well-characterized RHD, available in the GenBank database, are also included. The tree was constructed in MEGA X, and it involved a total of 59 sequences. (For interpretation of the references to colour in this figure legend, the reader is referred to the Web version of this article.)

the presence of B*a*A, in a similar effect to those observed for FT and PY on B*a*A degradation. The concentration of CHY did not start to decrease until day 15, but at that point, degradation of CHY started with kinetics significantly higher than those observed for CHY alone (26.4 ± 0.5 nmol kg^{-1}·day^{-1} and 9.1 ± 1.3 nmol kg^{-1}·day^{-1}, respectively). The observed sequential biodegradation of PAHs in the coincubations is consistent with their water solubility, as it is significantly higher for FT (0.26 mg/L) and PY (0.135 mg/L) than for B*a*A (0.009 mg/L), while B*a*A is more water soluble than CHY (0.002 mg/L). This effect is also in accordance with their tendency to sorb to the solid matrix of the soil, as the octanol-water partition coefficient of B*a*A is higher (log K_{ow} = 5.76) than that of FT and PY (5.16 and 4.88, respectively) but lower than that of CHY (5.81). However, the effect of other physicochemical parameters, such as chemical topology, cannot be disregarded. Then, the microbial populations of the creosote-contaminated soil would first degrade the more readily accessible PAHs, causing a delay in the removal of the less biodegradable compounds.

Previous studies on interactive effects during the biodegradation of PAH mixtures have been mainly addressed using pure bacterial cultures and, to a lesser extent, with defined consortia (Banerjee et al., 1995; Lotfabad & Gray, 2002; Mueller et al., 1989). These interactions may be synergistic, resulting in an increase in the degradation of one or more compounds, or inhibitory. Synergistic effects have been attributed to several factors, such as enhancement through biomass growth (Guha et al., 1999) or cross induction (Molina et al., 1999), but more frequently to cometabolic reactions, which are of special relevance in the biodegradation of HMW compounds (Jones et al., 2014). Conversely, inhibitory effects could also occur due to toxicity of the cosubstrate (Bouchez et al., 1995), the formation of toxic metabolites (Casellas et al., 1998; Ghosh & Mukherji, 2017), or the relaxed specificity and broad substrate range of the initial enzymes in PAH biodegradation pathways, which may lead to competitive inhibition (Stringfellow & Aitken, 1995; Dean-Ross et al., 2002; Desai et al., 2008). An alternative mechanism would control PAH degradation at the gene expression level via catabolite repression or induction of key enzymes. Facile degradation of a more soluble PAH could either repress enzymes for less accessible PAHs (Juhasz et al., 2002) or release metabolites to induce other pathways leading to cometabolic interactions (Rojo, 2021). All these interactive

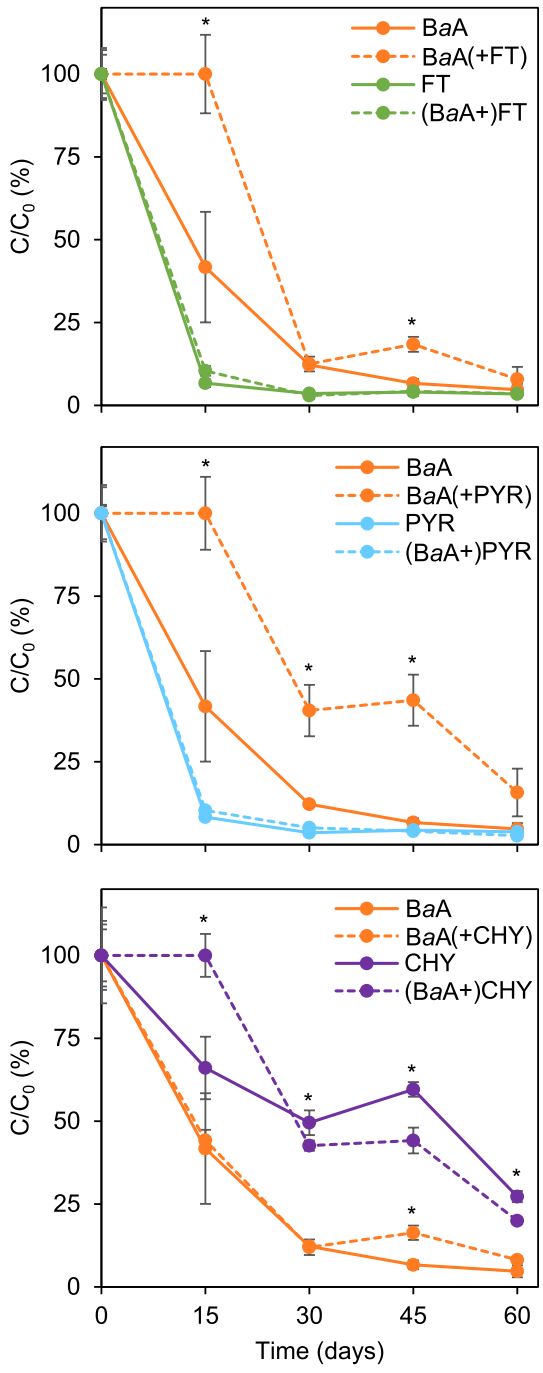

Fig. 3. Biodegradation kinetics of high molecular weight (HMW)-PAHs in the soil microcosms. C/C_0 indicates the relative concentration (%) at each incubation time with respect to the concentration at 0 days for each compound. B*a*A = benz(*a*)anthracene, FT = fluoranthene, PY = pyrene, CHY = chrysene, B*a*A(+FT) = B*a*A in the presence of FT; FT(+B*a*A) = FT in the presence of B*a*A; B*a*A(+PY) = B*a*A in the presence of PY; PY(+B*a*A) = PY in the presence of B*a*A; B*a*A(+CHY) = B*a*A in the presence of CHY; CHY(+B*a*A) = CHY in the presence of B*a*A. Each data point corresponds to the average of three replicates. Error bars represent the standard deviation. Asterisks indicate significant differences ($p < 0.05$) between individual and combined incubation of a specific substrate at a specific timepoint.

effects could explain the sequential selective biodegradation of PAHs in mixtures by single strains, ignoring other factors operating within complex soil microbial communities.

3.4. Relevant phylotypes in the biodegradation of single HMW-PAHs in soil microcosms

Analysis of the microbial community structure at the OTU level revealed a similar composition for all conditions, with a predominance of members of *Pseudoxanthomonas* (OTU 1, 24–40%), *Olivibacter* (OTU 2, 8–22%), *Pseudomonas* (OTU 3, 2.5–5%), *Phenylobacterium* (OTU 4, 3.8–6.4%), *Immundisolibacter* (OTU 5, 0.6–10.3%) and *Sphingomonas* (OTU 6, 1.8–5%). However, significant differences were observed for specific OTUs between microcosms (Figures S3, S4 and S5), indicating a differential enrichment associated with PAH assimilation. Analysis focused on those OTUs with >1% relative abundance in any library that experienced a significant increase over time. Statistical analyses of OTU relative abundances were performed in trios comparing the incubations containing B*a*A or the individual PAH cosubstrates alone and their coincubation at each incubation time (e.g., B*a*A alone versus FT alone versus B*a*A and FT together). In this manner, enrichment of each OTU could be associated with the degradation of either B*a*A, the cosubstrate or both. Additionally, a LEfSe analysis was performed to differentiate the OTUs explaining differences between all the conditions at each incubation time (Fig. 4).

OTUs associated with the biodegradation of B*a*A mainly belonged to members of *Olivibacter* (OTUs 2 and 11) at 15 days of incubation, *Immundisolibacter* (OTU 5) at 15 days and especially at 30 days, and to members of unclassified *Sphingomonadaceae* (OTU 12), *Sphingobium* (OTU 18) and *Luteimonas* (OTU 34) at 30 days. The LEfSe analysis revealed that *Olivibacter* (OTU 2) and *Immundisolibacter* (OTU 5) were the main OTUs responsible for the biodegradation of B*a*A, especially at 15 days of incubation. Members of the genus *Olivibacter* have been frequently found in contaminated environments (Villaverde et al., 2019); however, the reported isolates have been related to the utilization of monoaromatic intermediates in PAH metabolic pathways such as protocatechuate (Ntougias et al., 2007) or catechol (Ntougias et al., 2014), suggesting that it could utilize metabolites produced by other bacteria. On the other hand, the 16S rRNA sequence of OTU 5 matched at 100% identity with the sequence of *Immundisolibacter* sp. BA1, identified above as the key player in B*a*A degradation by DNA-SIP combined with shotgun metagenomics. For FT-containing microcosms, there was a remarkable increase in the relative abundance of OTU 8, classified as *Sphingobium*, and, to a minor extent, OTU 24, a member of *Mycobacterium*. The presence of *Actinobacteria*, although, was primarily associated with PY, with a prominent increase in *Mycobacterium* (OTU 24) and a slight increase in *Nocardiodes* (OTU 31) in microcosms containing this PAH. The relevance of *Mycobacterium* (OTU 24) in the degradation of PY was corroborated by LEfSe analysis. *Mycobacterium* is a well-investigated genus in the biodegradation of HMW-PAHs, particularly associated with pyrene and fluoranthene (Kweon et al., 2010). This genus has been recently divided into four novel genera, including the nonpathogenic genus *Mycolicibacterium*, which is related to PAH utilization (Gupta et al., 2018). *Pseudoxanthomonas* OTU 1, especially at 15 days, and a member of unclassified *Bacillaceae* (OTU 49) at 30 days, presented a significantly higher abundance in the presence of PY and CHY. The LEfSe analysis correlated *Pseudoxanthomonas* (OTU 1) to both PY (at 30 days) and CHY (at 15 days). Actually, the only two *Pseudoxanthomonas* isolates reported for PAH biodegradation were related to the utilization of pyrene (Klankeo et al., 2009) and chrysene (Nayak et al., 2011), indicating a potential role of this genus in the degradation of these HMW-PAHs.

3.5. Microbial interactions during BaA degradation in the presence of HMW-PAH cosubstrates

The analysis at the OTU level identified relevant microbial community interactions during the coincubation of B*a*A with other PAHs as cosubstrates. These interactions could probably be explained by cometabolic reactions, as ascertained from the analysis of the

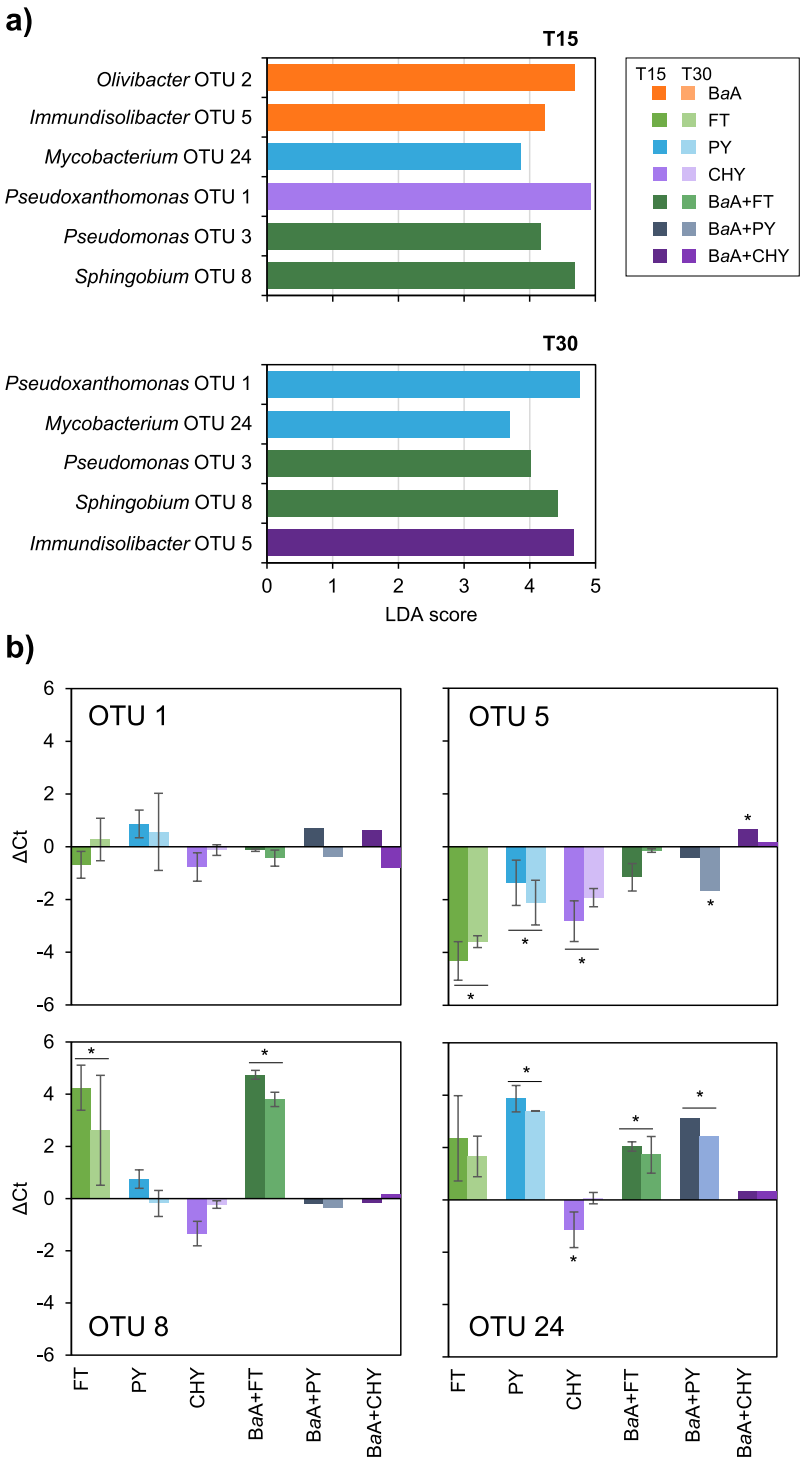

Fig. 4. (a) Linear discriminant analysis effect size (LEfSe) of the microbial community in the soil microcosms at OTU level at 15 (T15) and 30 (T30) days of incubation. Linear discriminant analysis (LDA) score is represented for OTUs with both, a significant increase ($p < 0.05$) during the incubation time and an LDA score >3.5. B*a*A = benz(*a*)anthracene; FT = fluoranthene; PY = pyrene; CHY = chrysene **(b)** Fold-change (ΔCt) of phylotype-specific 16S rRNA transcripts in the soil microcosms with respect to the microcosms with only B*a*A, quantified by qPCR analysis of cDNA samples. *Pseudoxanthomonas* OTU 1; *Immundisolibacter* OTU 5; *Sphingobium* OTU 8; *Mycobacterium* OTU 24. Values are the average and standard deviation of three replicates. Asterisks indicate significantly ($p < 0.05$) different Ct values compared to those of the microcosms with only B*a*A.

biodegradation kinetics. In the presence of FT, *Immundisolibacter* (OTU 5) and *Luteimonas* (OTU 34) experienced a significantly lower increase in abundance at 30 days of incubation compared to the incubations with B*a*A alone. In contrast, *Sphingobium* (OTU 8) and, to a lesser extent, an unclassified member of *Chitinophagaceae* (OTU 13) were significantly increased in the coincubation compared to any of the incubations with single substrates (either FT or B*a*A). In the LEfSe analysis, *Sphingobium* (OTU 8) was associated with the coincubation of FT and B*a*A. This result indicates that when FT was present, B*a*A degradation was partially channeled through these other members of the community. Considering that *Sphingobium* OTU 8 was identified as a major FT degrader, this could probably be attributed to a competition phenomenon, where *Sphingobium* OTU 8 would be favored by its overgrowth at the expense of FT. This enrichment of OTU 8 could also explain the increased degradation rates observed for B*a*A between 15 and 30 days during their coincubation. Sphingomonads are well known for their abilities to degrade a wide range of aromatic compounds, including HMW-PAHs, due to their great enzymatic versatility (Khara et al., 2014; Zhao et al., 2017). In fact, several *Sphingobium* strains have been found to cometabolize B*a*A in the presence of other PAHs; for example, *Sphingobium* sp. KK22, isolated from a phenanthrene enrichment culture of a bacterial consortium able to grow on diesel fuel, was capable of biotransforming B*a*A when grown

with phenanthrene (Kunihiro et al., 2013). Furthermore, the LEfSe analysis revealed a significant association of a member of *Pseudomonas* (OTU 3) with the coincubation of B*a*A and FT, suggesting a relevant role in the degradation of these two compounds.

When B*a*A was coincubated with PY, members of unclassified *Caulobacteraceae* (OTU 23) were enhanced at 15 days, and *Olivibacter* (OTU 2) remained dominant at 30 days. Similar to FT, when B*a*A and PY were together, *Immundisolibacter* (OTU 5) presented a significantly lower increase in its relative abundance compared to B*a*A individually. As suggested before, this could be associated with a possible utilization of B*a*A by other members of the microbial community; however, the extent of B*a*A degradation was lower in the presence of PY at 30 days, suggesting a possible inhibition of this specific OTU. The genus *Immundisolibacter* has been associated with the degradation of HMW-PAHs, particularly with PY (Singleton et al., 2006); nevertheless, OTU 5 did not seem to respond to the presence of PY alone, indicating a specialization of this particular phylotype in the degradation of B*a*A.

Conversely, for the coincubation of B*a*A with CHY, *Immundisolibacter* (OTU 5) experienced a remarkable increase at 30 days, reaching its maximum relative abundance considering all incubation conditions. This agreed with the LEfSe analysis, as OTU 5 was correlated with the coincubation of B*a*A and CHY. The increased abundance of this OTU coincided with a significantly higher degradation extent of CHY when coincubated with B*a*A. This synergistic effect of the presence of B*a*A on CHY degradation results from the action of *Immundisolibacter*.

The abundance of the total (16S rRNA genes) and active (16S rRNA transcripts) bacterial populations was quantified by qPCR. Overall, bacterial abundance and activity significantly increased after 15 days of incubation for all microcosms, going from $1.8{\cdot}10^8$ to 10^9 gene copies·g of dry soil^{-1} and from $8.2{\cdot}10^6$ to 10^8 transcript copies·g of dry soil^{-1}, respectively, and remained at the same level after 30 days. The relevance of *Pseudoxantomonas* OTU 1, *Immundisolibacter* OTU 5, *Sphingobium* OTU 8 and *Mycobacterium* OTU 24 was assessed at a transcriptomic level by quantification of their specific 16S rRNA transcripts in the soil microcosms. To evaluate their relative contribution to B*a*A degradation, the specific activity of each phylotype in all incubations was compared to their activity in the incubation with B*a*A alone (Fig. 4b). The results were expressed as the average change in Ct values (ΔCt) with respect to the Ct in B*a*A incubations. *Pseudoxanthomonas* OTU 1 showed minor variations in activity for all incubations, with no differences between conditions. The relative activity of *Immundisolibacter* OTU 5 with respect to B*a*A was lower in all conditions, except for the coincubation with B*a*A and CHY. This result confirmed the synergistic effect of this mixture on *Immundisolibacter* OTU 5 activity and the decreased contribution of this OTU to B*a*A biodegradation when coincubated with FT or PY as cosubstrates. Analysis of *Sphingobium* OTU 8 16S rRNA transcripts revealed an increase in activity only in those microcosms spiked with FT, either alone or in the presence of B*a*A. This result confirmed the major contribution of *Sphingobium* OTU 8 to FT degradation. Finally, *Mycobacterium* OTU 24 presented the highest activity in microcosms spiked with either FT or PY, especially the latter. The transcriptomic assessment reinforced the findings from the 16S rRNA amplicon sequencing data, demonstrating that the increased abundance of specific OTUs in response to FT, PY or B*a*A correlated with their increased activity in those incubations. Additionally, transcriptomic data revealed that the presence of other PAHs modulated the activity of *Immundisolibacter* OTU 5 during B*a*A degradation. The activity of OTU 5 decreased in the presence of more readily degradable cosubstrates (FT and PY), while the presence of CHY resulted in increased activity, thus confirming the existence of competitive inhibition and synergistic phenomena during the degradation of PAH mixtures.

4. Conclusions

DNA-SIP combined with metagenomics identified the key role of members of *Immundisolibacter* in the degradation of the four-ring PAH benz(*a*)anthracene in our model creosote-contaminated soil. Mining other metagenomic surveys for *Immundisolibacter* sp. BA1 genes demonstrated the worldwide distribution of this genus in PAH-contaminated soils, suggesting that it can be a global major player in the fate of HMW-PAHs. Functional analysis of the *Immundisolibacter* sp. BA1 MAG revealed a vast number of aromatic RHD coding genes and a highly conserved catabolic cluster within the genus. The phylogenetic divergence of some *Immundisolibacter* RHDs suggests their high degree of specialization and, thus, the need for their consideration when monitoring PAH-degrading communities by means of functional screens (i.e., qPCR of RHD genes). Our work also reveals that substrate interactions observed during the degradation of PAH mixtures by complex microbial communities can originate from competitive interactions within PAH-degrading populations. Members of *Immundisolibacter* were outcompeted by FT and PY degraders, while their action was enhanced in the presence of CHY. Similarly, members of *Sphingobium* were favored by the co-occurrence of FT and B*a*A. As a result, we observed a sequential degradation of HMW-PAHs in binary mixtures, with a major delay in the removal of the less biodegradable PAHs. This demonstrates that microbial interactive processes operate in the preferential utilization of PAHs in mixtures. These interactions should be considered when exploring the fate of HMW-PAHs in soils.

Credit author statement

Sara N. Jiménez-Volkerink: conceptualization, methodology, formal analysis, investigation, data curation, writing-original draft, visualization. **Maria Jordán:** investigation, formal analysis, visualization. **David Singleton:** methodology, formal analysis, resources. **Magdalena Grifoll:** conceptualization, methodology, resources, writing-review and editing, supervision, project administration, funding acquisition. **Joaquim Vila:** conceptualization, methodology, formal analysis, investigation, resources, writing-review and editing, supervision, project administration, funding acquisition.

Declaration of competing interest

The authors declare that they have no known competing financial interests or personal relationships that could have appeared to influence the work reported in this paper.

Data availability

All the accesion numbers to the databases where relevant sequencing data have been deposited can be found in the Material and Methods Section.

Acknowledgements

The authors are grateful to Prof. Michael D. Aitken for his guidance, contribution to the work and inestimable discussions. This work received funding from the Spanish Ministry of Science and Innovation, grant number PID 2019-109700RB-C22. SNJV was supported by an FPU fellowship (grant number FPU15/06077) of the Spanish Ministry of Education, Culture and Sports. MJ is supported by an FPI fellowship (grant number PRE 2020-093013) funded by the Spanish Ministry of Science and Innovation. JV is a Serra Húnter Fellow (Generalitat de Catalunya). The authors are members of the Water Research Institute from the University of Barcelona (IdRA-UB).

Appendix A. Supplementary data

Supplementary data to this article can be found online at https://doi.org/10.1016/j.envpol.2023.121624.

References

Baboshin, M., Akimov, V., Baskunov, B., Born, T.L., Khan, S.U., Golovleva, L., 2008. Conversion of polycyclic aromatic hydrocarbons by *Sphingomonas* sp. VKM B-2434. Biodegradation 19 (4), 567–576. https://doi.org/10.1007/s10532-007-9162-2.

Banerjee, D.K., Fedorak, P.M., Hashimoto, A., Masliyah, J.H., Pickard, M.A., Gray, M.R., 1995. Monitoring the biological treatment of anthracene-contaminated soil in a rotating-drum bioreactor. Appl. Microbiol. Biotechnol. 43 (3), 521–528. https://doi.org/10.1007/BF00218460.

Bastiaens, L., Springael, D., Wattiau, P., Harms, H., DeWachter, R., Verachtert, H., Diels, L., 2000. Isolation of adherent polycyclic aromatic hydrocarbon (PAH)-degrading bacteria using PAH-sorbing carriers. Appl. Environ. Microbiol. 66 (5), 1834–1843. https://doi.org/10.1128/AEM.66.5.1834-1843.2000.

Bolger, A.M., Lohse, M., Usadel, B., 2014. Trimmomatic: a flexible trimmer for Illumina sequence data. Bioinformatics 30 (15), 2114. https://doi.org/10.1093/BIOINFORMATICS/BTU170.

Bouchez, M., Blanchet, D., Vandecasteele, J.P., 1995. Degradation of polycyclic aromatic hydrocarbons by pure strains and by defined strain associations: inhibition phenomena and cometabolism. Appl. Microbiol. Biotechnol. 43 (1), 156–164. https://doi.org/10.1007/BF00170638.

Caporaso, J.G., Lauber, C.L., Walters, W.A., Berg-Lyons, D., Lozupone, C.A., Turnbaugh, P.J., Fierer, N., Knight, R., 2011. Global patterns of 16S rRNA diversity at a depth of millions of sequences per sample. Proc. Natl. Acad. Sci. USA 108 (Suppl. ment_1), 4516–4522. https://doi.org/10.1073/pnas.1000080107.

Casellas, M., Grifoll, M., Sabaté, J., Solanas, A.M., 1998. Isolation and characterization of a 9-fluorenone-degrading bacterial strain and its role in synergistic degradation of fluorene by a consortium. Can. J. Microbiol. 44 (8), 734–742. https://doi.org/10.1139/w98-066.

Chaumeil, P.A., Mussig, A.J., Hugenholtz, P., Parks, D.H., 2020. GTDB-Tk: a toolkit to classify genomes with the Genome Taxonomy Database. Bioinformatics 36 (6), 1925–1927. https://doi.org/10.1093/BIOINFORMATICS/BTZ848.

Cole, J.R., Wang, Q., Fish, J.A., Chai, B., McGarrell, D.M., Sun, Y., Brown, C.T., Porras-Alfaro, A., Kuske, C.R., Tiedje, J.M., 2014. Ribosomal Database Project: data and tools for high throughput rRNA analysis. Nucleic Acids Res. 42, D633. https://doi.org/10.1093/NAR/GKT1244. Database issue.

Corteselli, E.M., Aitken, M.D., Singleton, D.R., 2017. Description of *Immundisolibacter cernigliae* gen. nov., sp. nov., a high-molecular-weight polycyclic aromatic hydrocarbon-degrading bacterium within the class Gammaproteobacteria, and proposal of *Immundisolibacterales* ord. nov. and *Immundisolibacteraceae* f. Int. J. Syst. Evol. Microbiol. 67 (4), 925–931. https://doi.org/10.1099/ijsem.0.001714.

Dean-Ross, D., Moody, J., Cerniglia, C.E., 2002. Utilization of mixtures of polycyclic aromatic hydrocarbons by bacteria isolated from contaminated sediment. FEMS (Fed. Eur. Microbiol. Soc.) Microbiol. Ecol. 41 (1), 1–7. https://doi.org/10.1016/S0168-6496(02)00198-8.

Desai, A.M., Autenrieth, R.L., Dimitriou-Christidis, P., McDonald, T.J., 2008. Biodegradation kinetics of select polycyclic aromatic hydrocarbon (PAH) mixtures by *Sphingomonas paucimobilis* EPA505. Biodegradation 19 (2), 223–233. https://doi.org/10.1007/s10532-007-9129-3.

Duarte, M., Jauregui, R., Vilchez-Vargas, R., Junca, H., Pieper, D.H., 2014. AromaDeg, a novel database for phylogenomics of aerobic bacterial degradation of aromatics. Database 2014, 1–12. https://doi.org/10.1093/DATABASE/BAU118.

Duarte, M., Nielsen, A., Camarinha-Silva, A., Vilchez-Vargas, R., Bruls, T., Wos-Oxley, M. L., Jauregui, R., Pieper, D.H., 2017. Functional soil metagenomics: elucidation of polycyclic aromatic hydrocarbon degradation potential following 12 years of in situ bioremediation. Environ. Microbiol. 19 (8), 2992–3011. https://doi.org/10.1111/1462-2920.13756.

Ghosal, D., Ghosh, S., Dutta, T.K., Ahn, Y., 2016. Current state of knowledge in microbial degradation of polycyclic aromatic hydrocarbons (PAHs). Fron Microbiol. 7 (Issue AUG) https://doi.org/10.3389/fmicb.2016.01369. Front Media S.A.

Ghosh, I., Mukherji, S., 2017. Substrate interaction effects during pyrene biodegradation by *Pseudomonas aeruginosa* RS1. J. Environ. Chem. Eng. 5 (2), 1791–1800. https://doi.org/10.1016/j.jece.2017.03.016.

Grifoll, M., Selifonov, S.A., Gatlin, C.V., Chapman, P.J., 1995. Actions of a versatile fluorene-degrading bacterial isolate on polycyclic aromatic compounds. Applied and Environmental Microbiology 61 (10), 3711–3723. https://doi.org/10.1128/aem.61.10.3711-3723.1995.

Guha, S., Peters, C.A., Jaffé, P.R., 1999. Multisubstrate biodegradation kinetics of naphthalene, phenanthrene, and pyrene mixtures. Biotechnol. Bioeng. 65 (5), 491–499. https://doi.org/10.1002/(SICI)1097-0290(19991205)65:5<491::AID-BIT1>3.0.CO;2-H.

Gupta, R.S., Lo, B., Son, J., 2018. Phylogenomics and comparative genomic studies robustly support division of the genus *Mycobacterium* into an emended genus *Mycobacterium* and four novel genera. Front. Microbiol. 0 (FEB), 67. https://doi.org/10.3389/FMICB.2018.00067.

Jerina, D.M., Van Bladeren, P.J., Yagi, H., Gibson, D.T., Mahadevan, V., Neese, A.S., Koreeda, M., Sharma, N.D., Boyd, D.R., 1984. Synthesis and absolute configuration of the bacterial cis-1,2-, cis-8,9-, and cis-10,11-dihydro diol metabolites of benz[*a*]anthracene formed by strain of *Beijerinckia*. J. Org. Chem. 49 (19), 3621–3628. https://doi.org/10.1021/jo00193a033.

Jones, M.D., Crandell, D.W., Singleton, D.R., Aitken, M.D., 2011. Stable-isotope probing of the polycyclic aromatic hydrocarbon-degrading bacterial guild in a contaminated soil. Environ. Microbiol. 13 (10), 2623–2632. https://doi.org/10.1111/j.1462-2920.2011.02501.x.

Jones, M.D., Rodgers-Vieira, E.A., Hu, J., Aitken, M.D., 2014. Association of growth substrates and bacterial genera with benzo[*a*]pyrene mineralization in contaminated soil. Environ. Eng. Sci. 31 (12), 689. https://doi.org/10.1089/EES.2014.0275.

Jones, M.D., Singleton, D.R., Carstensen, D.P., Powell, S.N., Swanson, J.S., Pfaender, F. K., Aitken, M.D., 2008. Effect of incubation conditions on the enrichment of pyrene-degrading bacteria identified by stable-isotope probing in an aged, PAH-contaminated soil. Microb. Ecol. 56 (2), 341–349. https://doi.org/10.1007/s00248-007-9352-9.

Jouanneau, Y., Meyer, C., Duraffourg, N., 2016. Dihydroxylation of four- and five-ring aromatic hydrocarbons by the naphthalene dioxygenase from *Sphingomonas* CHY-1. Appl. Microbiol. Biotechnol. 100 (3), 1253–1263. https://doi.org/10.1007/s00253-015-7050-y.

Jouanneau, Y., Micoud, J., Meyer, C., 2007. Purification and characterization of a three-component salicylate 1-hydroxylase from *Sphingomonas* sp. strain CHY-1. Appl. Environ. Microbiol. 73 (23), 7515. https://doi.org/10.1128/AEM.01519-07.

Juhasz, A., Stanley, G., Britz, M., 2002. Metabolite repression inhibits degradation of benzo[*a*]pyrene and dibenz[*a,h*]anthracene by *Stenotrophomonas maltophilia* VUN 10,003. J. Ind. Microbiol. Biotechnol. 28 (2), 88–96. https://doi.org/10.1038/SJ/JIM/7000216.

Kanaly, R.A., Harayama, S., 2000. Biodegradation of high-molecular-weight polycyclic aromatic hydrocarbons by bacteria. J. Bacteriol. 182 (8), 2059–2067. https://doi.org/10.1128/JB.182.8.2059-2067.2000.

Kanaly, R.A., Harayama, S., 2010. Advances in the field of high-molecular-weight polycyclic aromatic hydrocarbon biodegradation by bacteria. Microb. Biotechnol. 3 (2), 136–164. https://doi.org/10.1111/j.1751-7915.2009.00130.x.

Khara, P., Roy, M., Chakraborty, J., Ghosal, D., Dutta, T.K., 2014. Functional characterization of diverse ring-hydroxylating oxygenases and induction of complex aromatic catabolic gene clusters in *Sphingobium* sp. PNB. FEBS Open Bio 4, 290–300. https://doi.org/10.1016/j.fob.2014.03.001.

Kim, S.J., Kweon, O., Freeman, J.P., Jones, R.C., Adjei, M.D., Jhoo, J.W., Edmondson, R. D., Cerniglia, C.E., 2006. Molecular cloning and expression of genes encoding a novel dioxygenase involved in low- and high-molecular-weight polycyclic aromatic hydrocarbon degradation in *Mycobacterium vanbaalenii* PYR-1. Appl. Environ. Microbiol. 72 (2), 1045–1054. https://doi.org/10.1128/AEM.72.2.1045-1054.2006.

Klankeo, P., Nopcharoenkul, W., Pinyakong, O., 2009. Two novel pyrene-degrading *Diaphorobacter* sp. and *Pseudoxanthomonas* sp. isolated from soil. J. Biosci. Bioeng. 108 (6), 488–495. https://doi.org/10.1016/j.jbiosc.2009.05.016.

Kozich, J.J., Westcott, S.L., Baxter, N.T., Highlander, S.K., Schloss, P.D., 2013. Development of a dual-index sequencing strategy and curation pipeline for analyzing amplicon sequence data on the miseq illumina sequencing platform. Appl. Environ. Microbiol. 79 (17), 5112–5120. https://doi.org/10.1128/AEM.01043-13.

Kunihiro, M., Ozeki, Y., Nogi, Y., Hamamura, N., Kanaly, R.A., 2013. Benz[*a*]anthracene biotransformation and production of ring fission products by *Sphingobium* sp. strain KK22. Appl. Environ. Microbiol. 79 (14), 4410–4420. https://doi.org/10.1128/AEM.01129-13.

Kweon, O., Kim, S.J., Freeman, J.P., Song, J., Baek, S., Cerniglia, C.E., 2010. Substrate specificity and structural characteristics of the novel Rieske nonheme iron aromatic ring-hydroxylating oxygenases NidAB and NidA3B3 from *Mycobacterium vanbaalenii* PYR-1. mBio 1 (2). https://doi.org/10.1128/MBIO.00135-10.

Langmead, B., Salzberg, S.L., 2012. Fast gapped-read alignment with Bowtie 2. Nature Methods. 9 (4), 357–359. https://doi.org/10.1038/NMETH.1923.

Lotfabad, S.K., Gray, M.R., 2002. Kinetics of biodegradation of mixtures of polycyclic aromatic hydrocarbons. Appl. Microbiol. Biotechnol. 60 (3), 361–365. https://doi.org/10.1007/s00253-002-1104-7.

Mahaffey, W.R., Gibson, D.T., Cerniglia, C.E., 1988. Bacterial oxidation of chemical carcinogens: formation of: polycyclic aromatic acids from benz[*a*]anthracene. Appl. Environ. Microbiol. 54 (10), 2415–2423. https://doi.org/10.1128/AEM.54.10.2415-2423.1988.

Matsumura, Y., Hosokawa, C., Sasaki-Mori, M., Akahira, A., Fukunaga, K., Ikeuchi, T., Oshiman, K.I., Tsuchido, T., 2009. Isolation and characterization of novel bisphenol -a-degrading bacteria from soils. Biocontrol Sci. 14 (4), 161–169. https://doi.org/10.4265/bio.14.161.

Molina, M., Araujo, R., Hodson, R.E., 1999. Cross-induction of pyrene and phenanthrene in a *Mycobacterium* sp. Isolated from polycyclic aromatic hydrocarbon contaminated river sediments. Can. J. Microbiol. 45 (6), 520–529. https://doi.org/10.1139/cjm-45-6-520.

Moody, J.D., Freeman, J.P., Cerniglia, C.E., 2005. Degradation of benz[*a*]anthracene by *Mycobacterium vanbaalenii* strain PYR-1. Biodegradation 16 (6), 513–526. https://doi.org/10.1007/s10532-004-7217-1.

Mueller, J.G., Chapman, P.J., Pritchard, P.H., 1989. Action of a fluoranthene-utilizing bacterial community on polycyclic aromatic hydrocarbon components of creosote. Appl. Environ. Microbiol. 55 (12), 3085–3090. https://doi.org/10.1128/aem.55.12.3085-3090.1989.

Muyzer, G., de Waal, E.C., Uitterlinden, A.G., 1993. Profiling of complex microbial populations by denaturing gradient gel electrophoresis analysis of polymerase chain reaction-amplified genes coding for 16S rRNA. Appl. Environ. Microbiol. 59 (3), 695–700. https://doi.org/10.1128/aem.59.3.695-700.1993.

Nayak, A.S., Sanjeev Kumar, S., Santosh Kumar, M., Anjaneya, O., Karegoudar, T.B., 2011. A catabolic pathway for the degradation of chrysene by *Pseudoxanthomonas* sp. PNK-04. FEMS (Fed. Eur. Microbiol. Soc.) Microbiol. Lett. 320 (2), 128–134. https://doi.org/10.1111/j.1574-6968.2011.02301.x.

Ntougias, S., Fasseas, C., Zervakis, G.I., 2007. *Olivibacter sitiensis* gen. nov., sp. nov., isolated from alkaline olive-oil mill wastes in the region of Sitia, Crete. Int. J. Syst. Evol. Microbiol. 57 (2), 398–404. https://doi.org/10.1099/ijs.0.64561-0.

Ntougias, S., Lapidus, A., Han, J., Mavromatis, K., Pati, A., Chen, A., Klenk, H.-P., Woyke, T., Fasseas, C., Kyrpides, N.C., Zervakis, G.I., 2014. High quality draft genome sequence of *Olivibacter sitiensis* type strain (AW-6T), a diphenol degrader with genes involved in the catechol pathway. Stand.Genom.Sci. 9 (3), 783–793. https://doi.org/10.4056/SIGS.5088950.

Nurk, S., Meleshko, D., Korobeynikov, A., Pevzner, P.A., 2017. MetaSPAdes: a new versatile metagenomic assembler. Genome Res. 27 (5), 824–834. https://doi.org/10.1101/GR.213959.116/-/DC1.

Parks, D.H., Imelfort, M., Skennerton, C.T., Hugenholtz, P., Tyson, G.W., 2015. CheckM: assessing the quality of microbial genomes recovered from isolates, single cells, and metagenomes. Genome Res. 25 (7), 1043. https://doi.org/10.1101/GR.186072.114.

Quast, C., Pruesse, E., Yilmaz, P., Gerken, J., Schweer, T., Yarza, P., Peplies, J., Glöckner, F.O., 2013. The SILVA ribosomal RNA gene database project: improved data processing and web-based tools. Nucleic Acids Res. 41 (D1), D590–D596. https://doi.org/10.1093/NAR/GKS1219.

Rojo, F., 2021. A new global regulator that facilitates the co-metabolization of polyaromatic hydrocarbons and other nutrients in *Novosphingobium*. Environ. Microbiol. 23 (6), 2875–2877. https://doi.org/10.1111/1462-2920.15527.

Schloss, P.D., Westcott, S.L., Ryabin, T., Hall, J.R., Hartmann, M., Hollister, E.B., Lesniewski, R.A., Oakley, B.B., Parks, D.H., Robinson, C.J., Sahl, J.W., Stres, B., Thallinger, G.G., Van Horn, D.J., Weber, C.F., 2009. Introducing mothur: open-source, platform-independent, community-supported software for describing and comparing microbial communities. Appl. Environ. Microbiol. 75 (23), 7537–7541. https://doi.org/10.1128/AEM.01541-09.

Seemann, T., 2014. Prokka: rapid prokaryotic genome annotation. Bioinformatics 30 (14), 2068–2069. https://doi.org/10.1093/BIOINFORMATICS/BTU153.

Segata, N., Izard, J., Waldron, L., Gevers, D., Miropolsky, L., Garrett, W.S., Huttenhower, C., 2011. Metagenomic biomarker discovery and explanation. Genome Biol. 12 (6), R60. https://doi.org/10.1186/gb-2011-12-6-r60.

Singh, A., Lal, R., 2009. *Sphingobium ummariense* sp. nov., a hexachlorocyclohexane (HCH)-degrading bacterium, isolated from HCH-contaminated soil. Int. J. Syst. Evol. Microbiol. 59 (1), 162–166. https://doi.org/10.1099/ijs.0.65712-0.

Singleton, D.R., Dickey, A.N., Scholl, E.H., Wright, F.A., Aitken, M.D., 2016. Complete genome sequence of a bacterium representing a deep uncultivated lineage within the Gammaproteobacteria associated with the degradation of polycyclic aromatic hydrocarbons. Genome Announc. 4 (5), 4–5. https://doi.org/10.1128/genomeA.01086-16.

Singleton, D.R., Sangaiah, R., Gold, A., Ball, L.M., Aitken, M.D., 2006. Identification and quantification of uncultivated Proteobacteria associated with pyrene degradation in a bioreactor treating PAH-contaminated soil. Environ. Microbiol. 8 (10), 1736–1745. https://doi.org/10.1111/j.1462-2920.2006.01112.x.

Sohn, J.H., Kwon, K.K., Kang, J.H., Jung, H.B., Kim, S.J., 2004. *Novosphingobium pentaromativorans* sp. nov., a high-molecular-mass polycyclic aromatic hydrocarbon-degrading bacterium isolated from estuarine sediment. Int. J. Syst. Evol. Microbiol. 54 (5), 1483–1487. https://doi.org/10.1099/ijs.0.02945-0.

Stringfellow, W.T., Aitken, M.D., 1995. Competitive metabolism of naphthalene, methylnaphthalenes, and fluorene by phenanthrene-degrading pseudomonads. Appl. Environ. Microbiol. 61 (1), 357–362. https://doi.org/10.1128/aem.61.1.357-362.1995.

Tian, Z., Gold, A., Nakamura, J., Zhang, Z., Vila, J., Singleton, D.R., Collins, L.B., Aitken, M.D., 2017. Nontarget analysis reveals a bacterial metabolite of pyrene implicated in the genotoxicity of contaminated soil after bioremediation. Environ. Sci. Technol. 51 (12), 7091–7100. https://doi.org/10.1021/acs.est.7b01172.

Tian, Z., Vila, J., Yu, M., Bodnar, W., Aitken, M.D., 2018. Tracing the biotransformation of polycyclic aromatic hydrocarbons in contaminated soil using stable isotope-assisted metabolomics. Environ. Sci. Technol. Lett. 5 (2), 103–109. https://doi.org/10.1021/acs.estlett.7b00554.

van der Oost, R., Beyer, J., Vermeulen, N.P., 2003. Fish bioaccumulation and biomarkers in environmental risk assessment: a review. Environ. Toxicol. Pharmacol. 13 (2), 57–149. https://doi.org/10.1016/S1382-6689(02)00126-6.

Vila, J., Tauler, M., Grifoll, M., 2015. Bacterial PAH degradation in marine and terrestrial habitats. Curr. Opin. Biotechnol. 33, 95–102. https://doi.org/10.1016/j.copbio.2015.01.006.

Villaverde, J., Láiz, L., Lara-Moreno, A., González-Pimentel, J.L., Morillo, E., 2019. Bioaugmentation of PAH-contaminated soils with novel specific degrader strains isolated from a contaminated industrial site. Effect of hydroxypropyl-β-cyclodextrin as PAH bioavailability enhancer. Front. Microbiol. 0, 2588. https://doi.org/10.3389/FMICB.2019.02588.

Wu, Y.W., Simmons, B.A., Singer, S.W., 2016. MaxBin 2.0: an automated binning algorithm to recover genomes from multiple metagenomic datasets. Bioinformatics 32 (4), 605–607. https://doi.org/10.1093/BIOINFORMATICS/BTV638.

Zhang, Z., Sangaiah, R., Gold, A., Ball, L.M., 2011. Synthesis of uniformly ^{13}C-labeled polycyclic aromatic hydrocarbons. Org. Biomol. Chem. 9 (15), 5431. https://doi.org/10.1039/c0ob01107j.

Zhao, Q., Yue, S., Bilal, M., Hu, H., Wang, W., Zhang, X., 2017. Comparative genomic analysis of 26 *Sphingomonas* and *Sphingobium* strains: dissemination of bioremediation capabilities, biodegradation potential and horizontal gene transfer. Sci. Total Environ. 609, 1238–1247. https://doi.org/10.1016/j.scitotenv.2017.07.249.